Chapter 1
Confocal Laser-scanning Microscopy in Filamentous Fungi

Rosa R. Mouriño-Pérez and Robert W. Roberson

1.1 Introduction

To answer many questions about how a fungal cell functions, it is necessary to examine cellular and subcellular events such as the behaviors and locations of specific organelles and proteins. For this purpose, there are a variety of fluorescence-imaging modalities that are commonly used, such as wide-field microscopy, laser-scanning confocal microscopy (LSCM) (Czymmek et al. 1994; Pawley 2006; Sheppard and Shotton 1997; Diaspro 2001), deconvolution microscopy (Panepinto et al. 2009; Swedlow 2003; Woyke et al. 2002), spinning-disk confocal microscopy (Ichiwara et al. 1999; Thorn 2010), two-photon microscopy (König 2000; Diaspro 2001; Feijo and Moreno 2004), and super-resolution microscopy methods (Huang et al. 2009; see Chap. 3). Confocal microscopy was developed in the 1950s (Minsky 1988). Though a working microscope was produced in 1955, the technological advances required to construct a practical research instrument delayed bringing it to market until the mid-1980s. Confocal microscopy has since become a widely used technique for imaging an extensive range of fluorescently labeled biological specimens, including fungi. Over the years, major improvements have been made in the technology applied in recording and displaying confocal images with high resolution and in determining the availability of more photo-stable fluorophores. Initially, confocal microscopy applications were used mainly in fixing images of fluorescently labeled specimens using, for example, immunofluorescence protocols. The imaging of living organisms has become more applicable to a wider range of specimens with the introduction

R. R. Mouriño-Pérez (✉)
Department of Microbiology, Center of Scientific Research and Higher Education of Ensenada, 3918 Carretera Ensenada-Tijuana, 22860 Ensenada, B. C., Mexico
e-mail: rmourino@cicese.mx

R. W. Roberson
School of Life Sciences, Arizona State University, Tempe, AZ, USA

T. E. S. Dahms and K. J. Czymmek (eds.), *Advanced Microscopy in Mycology,*
Fungal Biology, DOI 10.1007/978-3-319-22437-4_1

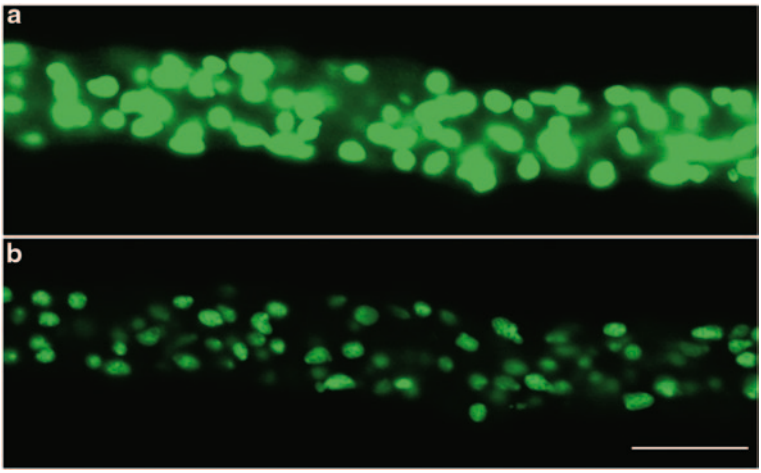

Fig. 1.1 Comparison of (**a**) a wide-field epifluorescence and (**b**) a confocal microscopy image of nuclei labeled with histone H1 fused to GFP in the filamentous fungus *Neurospora crassa*. Scale Bar = 10 μm. (Images by Olga A. Callejas-Negrete)

of fluorescent proteins, use of fluorescent vital dyes, and improved confocal systems (e.g., optics, light path, scanning strategies, and detector electronics) that have reduced photobleaching and phototoxicity. Live-cell imaging techniques provide a means for documenting organelle and macromolecular dynamics with increased spatial and temporal resolutions. Other advantages of confocal microscopy are the experimental approaches for multiple fluorescent labels and multidimensional microscopy.

The "optical section" is the basic image data obtained from a confocal microscope and refers to its ability to produce images along the z-axis (through the sample) of fluorescently-labeled specimens without resorting to physical sectioning of the sample (Fig. 1.1) that have higher contrast and resolution than images produced using a standard wide-field epifluorescence microscope (Conchello and Lichtman 2005; Chandler and Roberson 2009). Optical sections are produced in LSCM by scanning a region of interest of the specimen point-by-point with a focused laser beam, and using a pinhole aperture in front of the detector to remove out-of-focus fluorescent signal from above and below the focal plane of interest. Optical paths of confocal microscopy are designed in such a way that the laser beam is focused within the specimen and the resultant fluorescent signal is refocused at a pinhole in front of the detector (thus, the two focal points, making it confocal). The power of this approach lies in its ability to clearly image structures at discrete Z levels within an intact biological specimen.

1.2 The Confocal Microscopy System

The confocal microscopy system includes integrated optical and electronic devices such as a research grade microscope, multiple sources of coherent light (laser beams), a confocal scan head, a computer with one or two monitors and software

for image acquisition, processing and analysis (Fig. 1.2a). The essential part of the LSCM system is the scan head that directs input from one or more laser light sources, sets of filters that select excitation and emission wavelengths, a scanning mechanism, one or more pinhole apertures, and one or more photomultiplier tubes (PMT) as detectors for different fluorescent wavelengths (Fig. 1.2b).

Confocal microscopy was developed to remove out-of-focus light (haze) from the objective focal plane. How does it work?

First, the specimen must be illuminated with a specific wavelength of light to excite the fluorophore. Laser beams are used to illuminate the specimen through the objective lens, which is also a receptacle for the specimen-emitted light; thus, this lens functions as both a condenser and an objective. Dichroic mirrors, prisms, diffraction gratings, or tunable filters are used to obtain specific spectral excitation and/or emission signals. In LSCM, the laser beam fills the objective aperture and forms an intense diffraction-limited spot that is raster-scanned quickly from side to side and from top to bottom pixel by pixel across the entire specimen in a process called point-scanning.

As previously mentioned, the light emitted from the specimen is collected by the objective lens and then follows the microscope's optical path, reaching the pinhole aperture in front of the detector required to produce confocal images. The pinhole aperture is placed at a precise distance from the detector where the image-forming train of light is focused (Fig. 1.3; Chandler and Roberson 2009). The emitted light from a single optical plane within the specimen will pass directly through the center of the aperture. In contrast, light coming from specimen regions below and above the optical focal plane (i.e., out-of-focus) will focus before or after the aperture and are eliminated from the final image (Fig. 1.3; Paddock 2000, 2008; Foldes-Papp et al. 2003; Amos and White 2003; Pawley 2006; Murray et al. 2007). The size of the aperture, as well as the wavelength of exciting light and the NA of the objective lens will determine the resolution of the specimen's optical plane (Z thickness) that can be visualized, which is usually much smaller than the depth of focus for the objective lens (Chandler and Roberson 2009).

There are also alternative ways of collecting emitted light from the specimens when we are interested in a specific wavelength range ("user definable"). Emitted light can be separated into spectral bands using the method called spectral imaging, achieved by utilizing prisms, diffraction gratings, or tunable filters to obtain a specific spectral emission signal (Haraguchi et al. 2002; Czymmek 2005). Each fluorophore has a spectral fingerprint that can be obtained by collecting the emitted light intensity in a user-defined and specific total range that is acquiring images every 10 nm wavelength with a 500–650 nm spectral range. By plotting the intensity values in each image, it is possible to obtain the specific emission curve for the fluorophore of interest. It is possible to get the emission curve for as many fluorophores as needed. This information can be used to separate each spectra in multiple labeled specimens by a process called linear unmixing (Hiraoka et al. 2002; Czymmek 2005). Using spectral imaging it is possible to separate closely overlapping fluorophores and autofluorescence (Lin et al. 2009; Knaus et al. 2013).

Excitation and emission light paths are separated by a dichroic mirror or acousto–optic beam splitter before the light passes through the pinhole aperture to reach

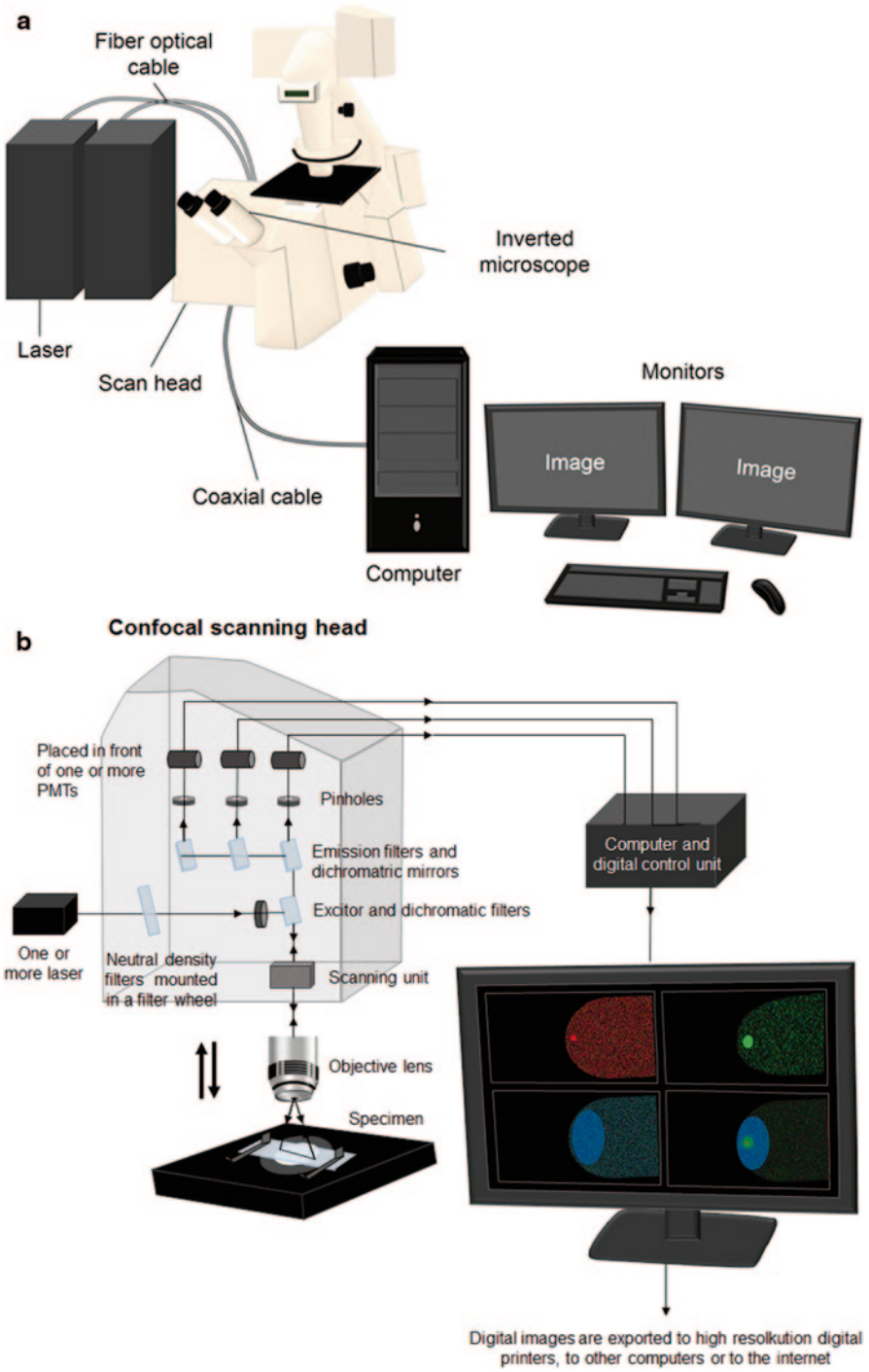

Fig. 1.2 Typical components of a laser-scanning confocal microscopy system. **a** Includes a research-grade microscope, upright or inverted, a scan head, laser beams, computer, and monitors. **b** Diagram of the confocal scanning head. It shows the laser input, the excitation filters and the emission filters, galvano mirrors and detectors. (Artwork by Arianne Ramirez-del Villar)

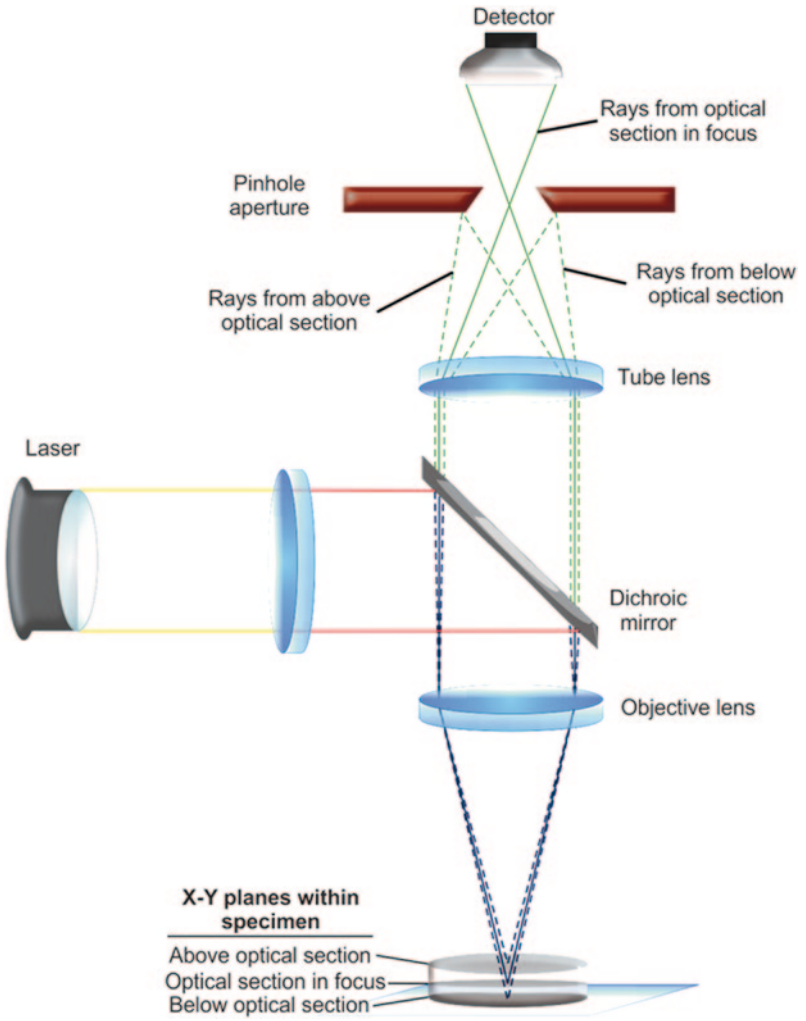

Fig. 1.3 Diagram of the light path in a confocal microscopy system. Pinhole aperture is in front of the detector in order to eliminate out-of-focus light. The image recorded therefore comes from one thin optical plane within the specimen (*solid line*) and the light above and below is blocked (*discontinuous line*). (Artwork by Fausto M. Villavicencio-Aguilar)

the scan head. The filtered light arrives at a galvano-scanning mirror that is constantly oscillating, and sends the signal to the detecting PMT or a more photon-sensitive GaAsP detector at an image plane in a wide-field fluorescence microscope (light path: filters-pinhole-Galvano mirror-detection device). The detectors do not perceive an image per se, but produce a voltage that corresponds to the intensity of incident light (photons) and the software digitizes the signal and displays it as an image on the monitor (Fig. 1.2b; Paddock 2000, 2008; Foldes-Papp et al. 2003; Amos and White 2003; Pawley 2006; Murray et al. 2007).

Each recorded image is an x–y point collection in a specific plane (z) within the specimen. To generate an image of the whole specimen, it is necessary to record an entire "stack" along the z-axis (Z stack) and use them to reconstruct the structure of the specimen with the aid of software that combines planes using mathematical algorithms (Chandler and Roberson 2009). Generally, the software is provided by and is proprietary to the manufacturer of the confocal system, though manufacturers allow export into common formats that can be used for third-party rendering/analysis software such as ImageJ.

1.3 Lasers

Confocal microscopy employs several types of lasers (diode lasers, diode-pumped solid state lasers, and noble gas ion lasers containing argon and helium–neon) to obtain the wavelengths required for fluorophore excitation across the ultraviolet and visible spectra, and to guarantee sufficient fluorescence intensity at the confocal pinhole (Table 1.1).

In the past, highly coherent and intense sources of light were generated by gas lasers (Svelto and Hanna 1989) that have been replaced by solid state lasers having superior performance, price, and longevity (Byer 1988; Wokosin et al. 1996; Kurtsiefer et al. 2000; Koechner 2006). Two important features of lasers used for advanced microscopy are their high degree of temporal coherence or monochromaticity (close to single wavelength) and the spatial coherence (the ability to produce a tight spot). The coherence length is the propagation distance over which a laser maintains a specified degree of coherence (Leith and Upatnieks 1963, 1964; Ackermann and Eichler 2007).

The light intensity profile of a laser beam is Gaussian. Thus, to have an even distribution of light intensity reach the objective, it is necessary to expand the excitation source such that it overfills both the field of view and condenser aperture. Laser speckle needs to be eliminated by reducing the coherence length of the laser beam to eliminate the interference from out-of-focus defects and at the image plane to maximize image resolution (Pawley 2010).

Table 1.1 Lasers used for confocal microscopy

Laser type	Wavelength (nm)				
Ultraviolet-argon	351, 364				
Argon-ion		458, 477, 488	515		
Krypton		488	568	647	
Helium–neon			543	633	
Diode	405	440, 473, 488	539, 559	638, 647	
Diode-pumped solid state	355, 405		532, 561	660, 671	1064
Titanium/sapphire					700–1000

1.4 Multidimensional Data Sets

An outstanding feature of confocal microscopy is the possibility of recording images in several dimensions, either sequentially or simultaneously; space (x, y, and z), time (Fig. 1.4) and emission wavelengths (channels), including non-confocal transmitted light images (Fig. 1.5). Thus, multidimensional images at different depths, time points, and/or multiple wavelengths can be presented as movies, including all or partial information. Different fluorophores can be imaged in a single multi-labeled specimen using a confocal system that combines multiple simultaneous excitation or conventional single-excitation sources. The limitation in the number of fluorophores imaged using the confocal approach is the ability to spectrally discriminate the emission spectra.

Multidimensional images collected by LSCM are usually in register with one another, facilitating their 3D display by computer reconstruction of the Z-series (Fig. 1.6) and the combination of multiwavelength images. Live cells are commonly imaged using time-lapse methods with the related data usually displayed as a time-lapse sequence directly from the confocal microscopy images (see below) (Waterman-Storer 1997).

1.5 Assessing Image Quality and the Performance of the Confocal System

The quality of a confocal image is determined by its spatial resolution, resolution of light intensity (dynamic range), signal-to-noise ratio (S/N), and temporal resolution (Pawley 2010).

Spatial resolution of a system is based on the minimum distance within two points can be distinguished as individual (Chandler and Roberson 2009), and which can be determined quantitatively. The numerical aperture (NA) of an objective and the illumination wavelength (lambda, λ) are crucial for spatial resolution. The minimum resolvable distance *d* between two points in the *x, y* plane can be approximated as (Pawley 2010):

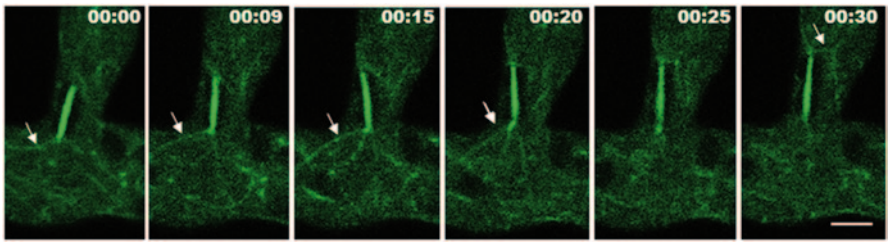

Fig. 1.4 Time lapse of a mitotic spindle in *Neurospora crassa* labeled with β-tubulin fused to GFP. *Arrows* point to astral microtubules. Time in min:sec. Scale bar = 10 μm

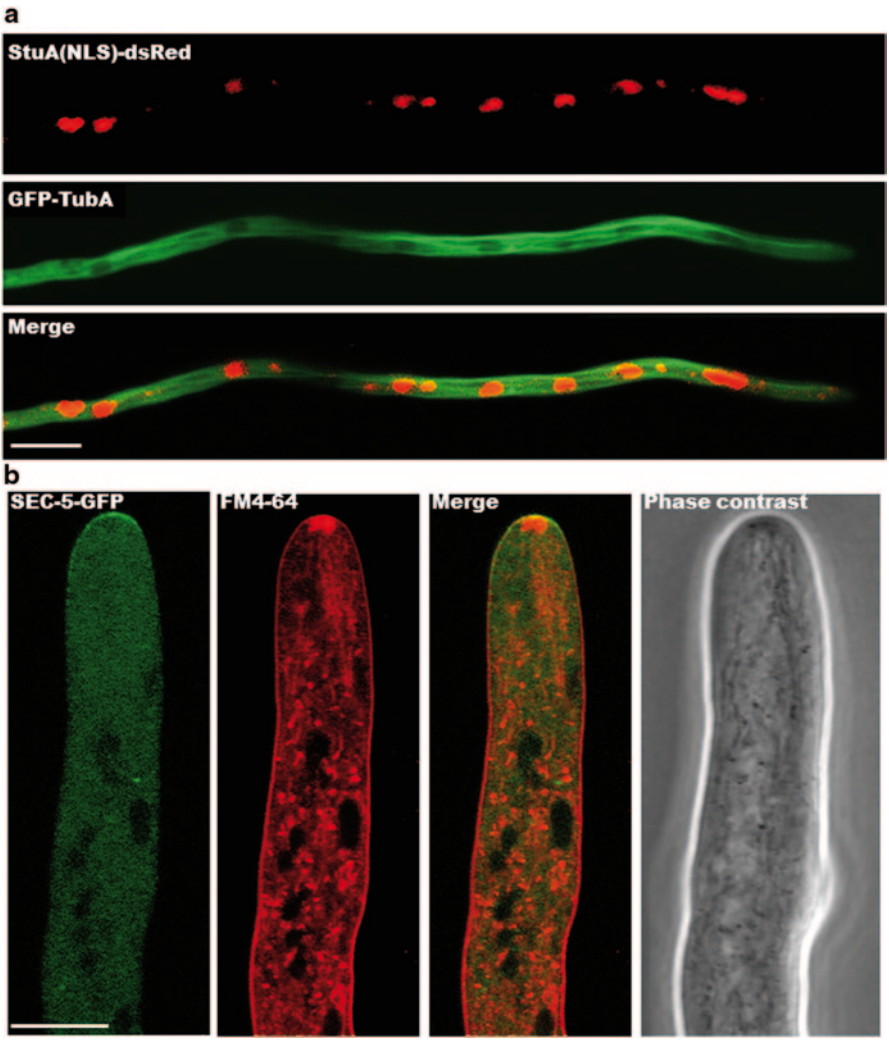

Fig. 1.5 Hyphae multilabeled with fluorescent proteins and vital dyes. **a** Panel 1, single hypha of *Aspergillus nidulans* showing nuclei labeled with StuA(NLS)-dsRed. Panel 2, same cell with microtubules labeled with GFP-TubA. Panel 3, merger of images in panels 1 and 2. Scale bar = 10 μm. (Images by Raphael Manck). **b** Panel 1, single hypha of *Neurospora crassa* labeled with SEC-5-GFP (exocyst component). Panel 2, membranes stained with the lipophilic vital dye FM4-64. Panel 3, merger of images in panels 1 and 2 and panel 3 phase contrast image. Scale bar = 10 μm. (Images by Alejandro Beltran and Meritxell Riquelme)

$$d_{x,y} \approx \frac{0.4\lambda}{\mathrm{NA}}.$$

It is important to use objectives with high NA when the goal is to increase the resolution, since NA is inversely proportional to d. Since NA is equal to $n \sin\theta$, where n is the refractive index and θ the angular aperture, the use of oil immersion (higher n)

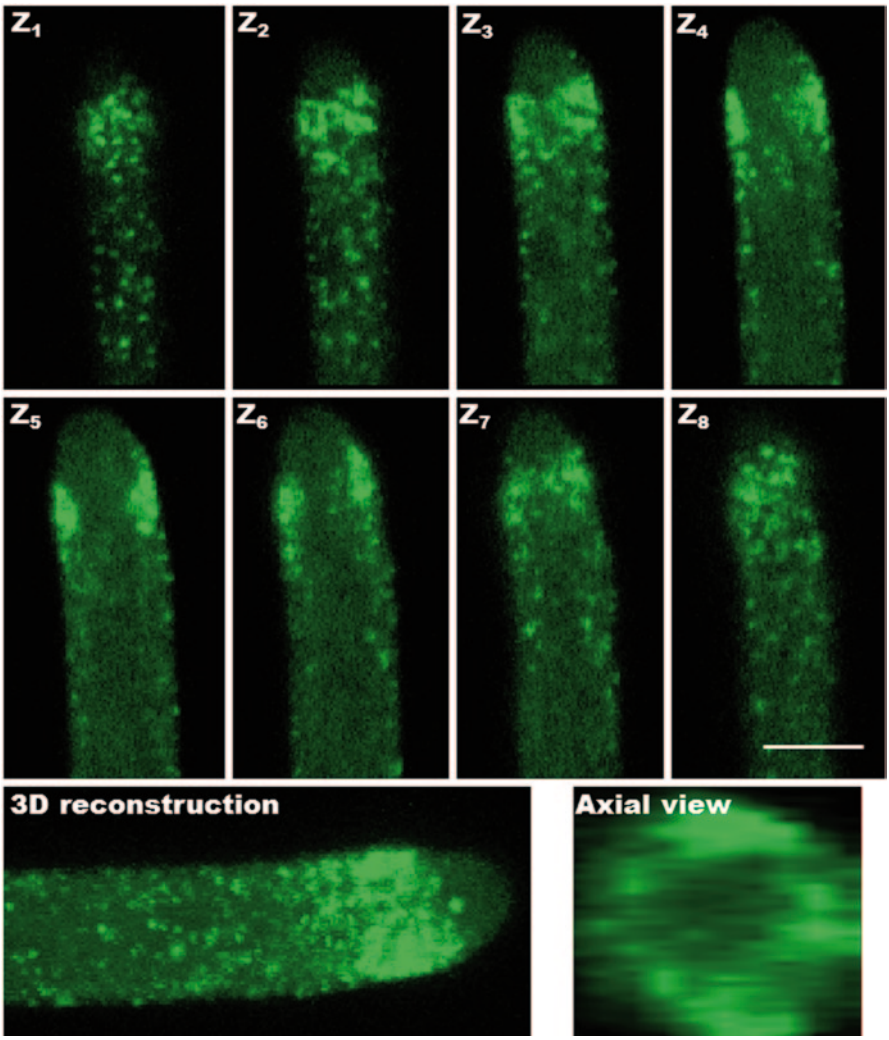

Fig. 1.6 3D reconstruction of the apical and subapical region of *Neurospora crassa* labeled with fimbrin fuse to GFP. ($Z_{1–8}$) single optical sections of 0.9 μm from top to botton of the hypha. *Bottom panel* in the left shows the reconstruction with all eight optical sections and the *right panel* shows an axial view of the reconstruction. Fimbrin forms a collar around the subapical region. Scale bar = 10 μm

improves resolution. Other factors that can affect spatial resolution are the size of the pinhole (reducing the size of the pinhole improves contrast by eliminating out-of-focus light, but reduces signal collection and thus image intensity), the zoom factor, pixel resolution, and the scan rate (by decreasing the field of view and the scan rate, the amount of light detected increases), all of which can be adjusted using the software (Pawley 2010).

On the detection side, the dynamic range refers to the resolution of light intensity and is defined as the ratio of saturated signal to detector readout noise, calculated in volts or electrons. In other words, the dynamic range can be defined as the number of gray levels that are assigned to an image by the analog-to-digital converter. To attain the maximal potential of the PMT, it is important to acquire images in a dynamic range from no signal (black) to saturating signal (white) (Murphy and Davidson 2013). The signal-to-noise (S/N) ratio, which directly affects image contrast, depends on specimen background and the electronic noise of the system.

Temporal resolution is another aspect for assessing image quality and the performance of a confocal system. Temporal resolution is occasionally a problem, particularly in older generation confocal microscopes. The use of modern resonant scanners and galvo scanner systems has greatly improved temporal resolution issues in confocal microscopy.

1.6 Pros and Cons of Confocal Microscopy

Of the types of microscopy capable of optical sectioning, LSCM has been the most popular. To apply this technique with maximum power and optimal results, it is important to know the associated pros and cons (Table 1.2) to plan experiments that will yield maximal information as answers to our experimental questions (Shotton 1989; Pawley 2010; Hickey and Read 2009).

Table 1.2 Pros and cons of confocal microscopy

Pros	Cons
The ability to optically section through fluorescent objects	Restriction of illuminating wavelengths
Reduction in background signal	Photobleaching
Stacking images representing different focal planes spaced at regular intervals along the optical axis (z-axis)	Relatively slow scan rates
Digitization by an analog to digital converter (transformation of continuous voltage signal into discrete digital steps of light intensity)	Requires associated digital image processor for optimum usefulness
Permits unusually clear examination of thick, light scattering objects	Use of a small confocal aperture reduces overall image intensity
Obtain high-contrast images of surface topologies	Out-of-focus structures invisible
Greatly improved S/N ratio	Bleed-through in fluorophores with similar spectra
Electronic adjustment of magnification	Relatively expensive
Reduce blurring of the image from light-scattering	

1.7 LSCM Advanced Techniques

There are different advanced LSCM techniques such as bimolecular complementation (BiFC), fluorescence recovery after photobleaching (FRAP), fluorescence loss in photobleaching (FLIP), fluorescence lifetime-imaging microscopy (FLIM), fluorescence resonance energy transfer (FRET) that are covered in Chap. 2. Other advanced techniques are fluorescence correlation spectroscopy (FCS) and fluorescence cross-correlation spectroscopy (FCCS), and biophysical techniques that provide quantitative measurements of important parameters, including mechanisms of molecular mobilities, and concentrations in living cells. *In vitro*, FCS examines the inherent correlations exhibited by the fluctuating fluorescent signal from labeled molecules as they transition into and out of a specified excitation volume or area. FCCS, an extension of FCS, measures the temporal fluorescence fluctuations coming from two differently labeled molecules diffusing through a small sample volume. It has become an important method for characterizing diffusion coefficients, binding constants, kinetic rates of binding, and determining molecular interactions (Krichevsky and Bonnet 2002; Baciaet al. 2006; Hwang and Wohland 2007; Tcherniak et al. 2009; Digman and Gratton 2009). Tsujia et al. (2011) used FCS and FCCS to track the two- and three-dimensional motion of quantum dot-conjugated prion proteins in cells of *Saccharomyces cerevisiae.* They developed a method that paved the way for tracking single proteins of interest inside living cells through recording and analyzing the stochastic behaviors of individual quantum dots.

1.8 Comparison of LSCM with Spinning-disc, Deconvolution and Two-Photon Methods

Over the past 70 years, a variety of confocal technologies similar to LSCM have been developed. Spinning-disk confocal (Ichiwara et al. 1999; Nakano 2002), deconvolution (Swedlow 2003), and two-photon confocal microscopy (König 2000; Diaspro 2001; Feijo and Moreno 2004) allow imaging living cells at high spatial resolution, in addition to optical sectioning.

Spinning-disk confocal microscopy is based on the use of the Yokogawa-Nipkow disc that is a combination of two discs, one with an appropriate pattern of pinholes of a fixed size (Nipkow) and the other containing the same pinhole pattern but with a microlens in each pinhole that focuses illuminating light to reduce diffraction-induced spread of the beam (Yokogawa) (Wang et al. 2005). The discs spin synchronously at 6000–8000 rpm, effectively creating a simultaneous illumination of the entire region of interest. Each pattern of pinholes returns to a given spot once per cycle, illuminating each spot for a longer amount of time overall thus reducing the excitation energy needed to illuminate a sample (Nakano 2002; Wang et al. 2005). Since excitation of any given spot is intermittent, phototoxicity and photobleaching of the specimen are reduced and temporal resolution enhanced,

which is advantageous for live samples that are delicate (Nakano 2002). Instead of the PMT detectors of LSCM, spinning-disc confocal microscopes use electron-multiplying charge-coupled device (EMCCD) detectors to record images, in addition to enhancing the temporal resolution (Nakano 2002). Excellent examples of the use of spinning-disc confocal microscopy in studying fungal cell biology include the relationship between dynamic microtubules and mitotic spindle poles with mitochondrial positioning in fission yeast (Yaffe et al. 2003), *Ustilago maydis* effector production during plant infection driven by long-distance endosome trafficking (Bielska et al. 2014), the clathrin- and Arp2/3-independent endocytosis in *Candida albicans* (Epp et al. 2013), the regulation of mitosis by the NIMA kinase present in spindle pole bodies of *Aspergillus nidulans*, the chronological appearance of each component of the kinase cascade (Shen and Osmani 2013), and microtubule dynamics during mitosis in *Aspergillus nidulans* (Szewczyk and Oakley 2011); in this study, they used spinning-disk confocal microscopy because it allowed rapid image capture. As microtubule dynamics are extremely rapid, it is necessary to use a fast acquisition system.

One of the major causes of image degradation in wide-field fluorescence microscopy is blurring caused by signals emanating from the out-of-focus fluorescence that would normally be eliminated by the confocal pinhole. This can also be overcome using a computer-based method commonly known as deconvolution microscopy in which deconvolution algorithms either subtract or reassign out-of-focus light. A variety of algorithms are now commercially available for 2D or 3D deconvolution (Wallace et al. 2001; Swedlow 2003; Nasse and Woehl 2010), most easily classified as non-restorative and restorative methods. The former improves contrast by removing out-of-focus light from focal planes, and the latter reassigns light to its proper place of origin. Such methods can be advantageous over 3D confocal microscopy since light is not discarded but rather reused. Images or time series for deconvolution microscopy are recorded by wide-field epifluorescence microcopy, and depending on the detection optics, the spatial and temporal resolution can be very high (Wallace et al. 2001; Swedlow 2003; Nasse and Woehl 2010). Deconvolution microscopy was used successfully in investigating the events of mitosis in *Cryptococcus neoformans* (Woyke et al. 2002), localizing the Rho-GTPase RHO-4 during conidiation versus vegetative septation in the filamentous fungus *Neurospora crassa* (Rasmussen and Glass 2007), understanding the components of the exocyst and polarisome in *Ashbya gossypii* (Köhli et al. 2008), studying the dynamic cellular processes such as growth, cell division, and morphogenesis in budding yeast (Rines et al. 2011) and mapping the yeast kinetochore (Haase et al. 2013); they deconvolved and background subtracted 13 planes, 200 nm apart, to make a 3-D reconstruction of the kinetochore of *Saccharomyces cerevisiae* during mitosis.

An additional imaging approach that can be applied to wide-field fluorescence or confocal microscopy is two- or multiphoton excitation. For two-photon excitation, the most commonly used fluorophores have excitation spectra of 350–500 nm, whereas the laser used for excitation is in the range of ~700–1000 nm (infrared). When a fluorophore absorbs two infrared photons simultaneously, it will absorb

enough energy to be raised to the excited state ($E = hc/\lambda$ wavelength is inversely proportional to energy). The fluorophore will emit a single photon with a wavelength that depends on the type of fluorophore used (typically in the visible spectrum). The two-photon method typically requires a pulsed femtosecond laser to quickly deliver photons at high density. The spatial and temporal resolution of two-photon fluorescence microscopy is very similar to LSCM and the two are commonly combined; however, the specialized laser makes it more expensive and slightly more difficult to use. Advantages of two-photon excitation include its superior depth of imaging (up to 1 mm) and minimal phototoxicity (lower energy excitation), making the system well suited for specimens of living organisms (Arcangeli et al. 2000; Czymmek 2005; Knaus et al. 2013). Multiphoton microscopy, with its increased depth of field, has made it possible to document *in vivo* the mechanisms of invasion into the *Arabidopsis root* vascular system by *Fusarium oxysporum* (Czymmek et al. 2007), the multiphoton imaging of medically significant fungi such as *Aspergillus flavus*, *Micosporum gypseum*, *Micosoprum canis*, *Trichophyton rubrum*, and *Trichophyton tonsurans* to analyze their distinct autofluorescence characteristics in microcultures in Sabouraud's agar. They showed that multiphoton microscopy is a powerful noninvasive tool in biomedical imaging. Multiphoton imaging advantages such as strong axial-depth discrimination, enhanced image penetration, and reduced photodamage were revealed to be useful in fungal morphological characterization. The authors showed that hyphae and spores are intensely autofluorescent, providing strong contrast. The fungal cell wall, cytoplasm, and septum were clearly seen. Each fungal species had distinct autofluorescence spectral fingerprints, and the analysis of the multiphoton fluorescence fingerprint could potentially help in differentiating fungal species (Lin et al. 2009).

1.9 Fungal Sample Preparation

With confocal microscopy, it is possible to observe fixed and living fungal specimens. Fixed cells are more robust than living cells, but offer less information about cellular dynamics (Chandler and Roberson 2009).

A common method to localize macromolecules in the context of fixed cells is immunocytochemistry, in which antibodies bind with a high degree of specificity to unique structural features (i.e., epitopes) on the surface of the macromolecules. Whole mount single cells (Hoch and Staples 1985; Roberson 1992; Bourett et al. 1998) or sections of sporangia or complex tissues (Hyde and Hardham 1992) can be prepared for immunocytochemistry with each approach requiring that epitope structural integrity be maintained sufficiently for antibody recognition. Typically, samples are chemically fixed in freshly prepared, buffered (e.g., phosphate-buffered saline) formaldehyde (4%w/v) for 30 min at room temperature, and then rinsed to remove the excess fixative. These samples can be stored at 4ºC for several days, but it is preferable if they are processed immediately. Samples can also be flash frozen using a variety of cryogens, such as cold (−15−85ºC) organic sol-

vents (e.g., methanol, acetone) (Bourett et al. 1998; Riquelme et al. 2002), or liquid nitrogen cooled propane (Lowry and Roberson 1997; McDaniel and Roberson 1998). After freezing, the samples are incubated in an appropriate solvent at −20 ºC overnight, warmed to 4 ºC, rehydrated in buffer and processed. Chemically fixed whole mount samples must be permeabilized to allow the diffusion of antibodies into and out of cells during incubation periods. Permeabilization is accomplished using enzyme(s) to partially digest the cell wall (e.g., chitinase) and a gentle detergent (triton X-100) to disrupt the plasma and cytosolic membranes. Disruption of the cell wall may be required for cryo-fixed samples, but detergent treatment is typically not required. Localization of the antigen is carried out indirectly by the use of two antibodies; the first (or primary) antibody localizes the antigen (target macromolecule) whereas the second (or secondary) antibody to the primary antibody is associated with the fluorophore. In order to minimize nonspecific antibody binding to the specimen, incubation in dilute, buffered protein (e.g., bovine serum albumin) is recommended. There are two primary advantages of the indirect approach: (1) a single primary antibody can be localized by multiple secondary antibodies, thus, enhancing signal and sensitivity, and (2) secondary antibodies can be conjugated to a wide choice of inexpensive fluorophores that are commercially available. Antibody dilution and incubation times must be determined empirically for each specimen; 1:100 or 1:1000 are typical dilutions. Following incubation with primary and secondary antibodies, samples are washed and mounted on clean glass slides in a volume of glycerol-based antifade reagent (e.g., n-propyl gallate), and overlaid with a glass cover slip. Samples are stored in the dark at 4 ºC until viewing, and sample preparation in the dark can prevent photobleaching of sensitive fluorophores (Chandler and Roberson 2009). Figure 1.7 shows examples of multi-labeled (antibodies and DAPI) fixed fungal hyphae. Some examples of confocal microscopy images of immunolocalization are localizing γ-tubulin as a component of the Spitzenkörper and centrosomes in *Allomyces macrogynus* (McDaniel and Roberson 1998), studying the microtubule cytoskeleton in association with vesicular and mitochondrial motility and positioning in the hyphal apex of *Allomyces macrogynus* (McDaniel and Roberson 2000), and identifying microtubules with detyrosinated α-tubulin and their exclusive motors (Kinesin-3 UncA) in *Aspergillus nidulans*. In this study, the authors showed different populations of microtubules, with just one detyrosinated α-tubulin microtubule in *A. nidulans* that is exclusively associated with Kinesin-3 (Zekert and Fischer 2009).

To maintain the health of cells during live-cell imaging, sample fluorophore concentrations are decreased to reduce cytotoxicity and laser irradiation minimized to prevent phototoxicity and photobleaching. Hickey and Read (2003) reported the "inverted agar block method" (Fig. 1.8) to maintain mycelium in a single focal plane and to reduce spherical aberration (Hickey et al. 2005; Hickey and Read 2009). This method involves cutting a ~2 × 3 cm agar rectangle from the margin of a fungal colony, growing it in an agar plate and leaving plenty of space for hyphae to grow (Fig. 1.8). When cells are labeled with fluorescent proteins, the agar block is placed inverted onto a glass coverslip without any liquid. If extrinsic fluorescent dyes are required, they must be added as ~10–20 µl drops of dye-containing liquid

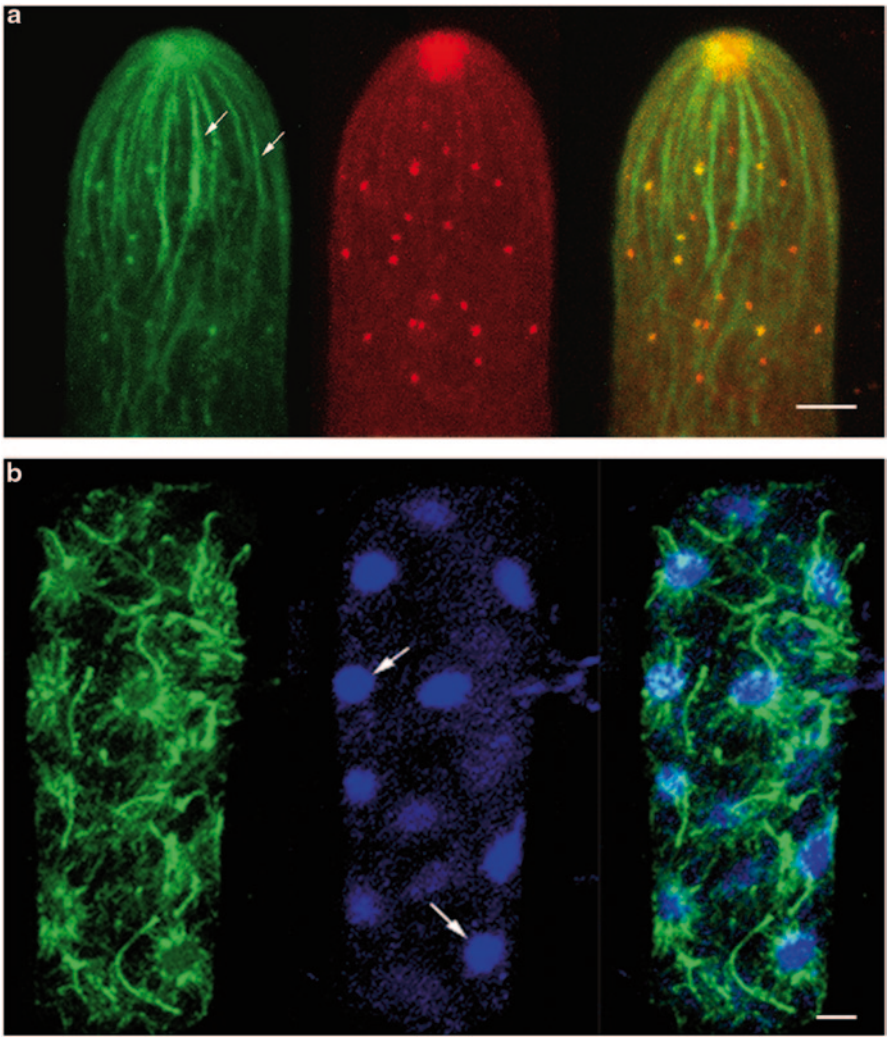

Fig. 1.7 Indirect immunofluorescence labeling of *Allomyces macrogynus* cells. **a** *Panel 1*. A single hyphal tip labeled for visualization of α-tubulin showing abundant microtubules (*arrows*) organized around and emanating from the hyphal apex. *Panel 2*. Same cell as seen in panel 1 showing γ-tubulin localized to a spherical region in the hyphal apex corresponding to the Spitzenkörper, and in the subapical cytoplasm as discrete spots corresponding to centrosomes. *Panel 3*. Merged image of *panels 1* and *2*. Scale bar = 2 μm (images by Dennis McDaniels). **b** *Panel 1*. A single zoosporangium undergoing zoosporogenesis labeled for α-tubulin localization showing extensive microtubule arrays. *Panel 2*, same sporangium shown in panel 1 labeled with DAPI for nuclear visualization (*arrows*). *Panel 3*, merged image of *panels 1* and 2. Scale bar = 10 μm. (Images by David Lowry)

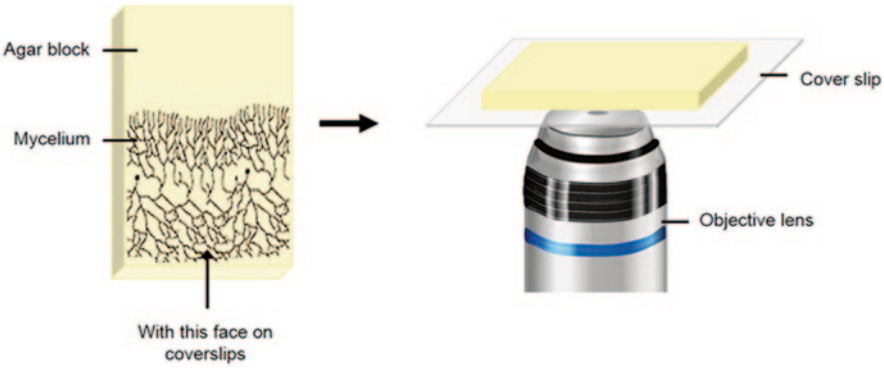

Fig. 1.8 Scheme of the "inverted agar block" developed by Hickey and Read (2003) for living-cell imaging in filamentous fungi

growth medium to the coverslip, before gently placing the agar block (Hickey et al. 2002). Preparation of hyphal cells in this way often results in cessation of growth, thus 10–20 min recovery time is typically required prior to imaging. For multi-labeled live hyphae, fluorescent dyes and proteins can be used in one organism. For instance, we can use GFP and mCherry (or dsRed) (Fig. 1.5) or a GFP labeled strain having FM4-64 stained membranes and calcofluor white stained cell walls. Examples of multi-labeled specimens are shown in the study of the actin cytoskeleton in *Neurospora crassa* during vegetative hyphal growth, where different actin reporters were used to localize the multiple actin-based structures and understand their function that is support and transport. Actin was labeled with the marker Lifeact-GFP (Riedl et al. 2008) and the actin-binding proteins (ABPs: fimbrin, Arp-2, Arp-3, and tropomyosin) that were associated with either GFP or mCherry. This study demonstrated the versatility of actin in both its location throughout the hypha and in its varied associations with ABPs, which regulate the construction-specific actin-based structures (Delgado-Alvarez et al. 2010). Using these methods it was also possible to draw a timeline for actin and ABPs during septum formation, using FM4-64 as the time marker for septation (Delgado-Alvarez et al. 2014). In the human pathogen *Candida albicans*, multi-labeled living hyphae have been useful to study different patterns of localization and distinct dynamic properties of the Spitzenkörper, exocyst, and polarisome components, and the phosphorylation of Exo84 by the cyclin Cdk1-Hgc1 during hyphal extension (Caballero-Lima and Sudbery 2014).

Table 1.3 presents some examples of the different dyes and fluorescent proteins available for fungal cells. Before starting any experiment, it is important to know the excitation and emission spectra of each fluorophore, which may change in the context of the organism. Thus, it is prudent to collect spectral scans of each fluorophore following labeling prior to conducting the confocal experiment. If dual or triple labeling is required, dyes must be chosen that have well-separated emission spectra. Sometimes, it is not possible to resolve the emission signal of fluorophores with similar spectra, and so dyes must be chosen carefully prior to imaging.

Table 1.3 Vital fluorophores and fluorescent proteins used in fugal cells

	Wavelength		
Fluorophore	Excitation	Emission	Target
FM4-64	488	515	Plasma and cytosolic membranes
$DIOC_6$	484	501	Mitochondria, endoplasmic reticulum, and nuclear envelope
DAPI	315	455	DNA and RNA
SYTO dyes	468	533	Nuclei and mitochondrial DNA
Rhodamine 123	507	530	Active mitochondria
DASPMI	475	605	Mitochondria
FM1-43	488	590	Mitochondria
Mitotracker red	644	665	Mitochondria
Rhodamine Phaloidine	540	565	Actin
Calcofluor white	365	490	Cell wall
Solophenyl flavine	440	530	Cell wall
Oregon green	498	526	Vacuoles
Lucifer yellow	428	540	Fluid-phase endocytosis
FITC-dextran	490	520	Fluid-phase endocytosis
Fluorescent proteins			
sGFP	485	510	
eGFP	489	508	
Venus	515	528	
YFP	514	527	
dsRed	556	589	
mCherry	587	610	
EOS	Variable		

Refences for Vital dyes: Johnson et al. 1980; Elorza et al. 1983; Roncero and Duran 1985; Betz et al. 1992, 1996; Knight et al. 1993; Oparka and Read 1994; Vida and Emr 1995; Hoffman and Mendgen 1998; Steinber et al. 1998; Cochilla et al. 1999; Bolte et al. 2004; Fisher-Parton et al. 2000; Read and Hickey 2001; Atkinson et al. 2002; Torralba and Heath 2002; Dijksterhuis 2003; Read and Kalkman 2003; Miyawaki 2003; Bolte et al. 2004; Koll et al. 2001. *References for Fluorescent proteins*: Freitag and Selker 2005; Freitag et al. 2001, 2004; Fuchs et al. 2002; Day and Davidson 2009; Bowman et al. 2009; Leroch et al. 2011.

1.10 Image Processing and Movie-making

Images acquired by LSCM are usually saved in a digital computer format that are easily converted to different file types for manipulation using the proprietary software of the confocal microscope or other commercially or freely available image processing software. It is possible to separate the different channels, time points, and/or the Z-stacks for 3-D reconstruction. Each single image can be converted to any format (e.g., jpg, tif, gif, etc.) depending of the quality desired, but the raw data should always be stored for future processing. Image brightness, contrast, cropping, and/or merging is generally accomplished using image processing software such as Adobe Photoshop®. It is important not to over-manipulate images, thereby, avoiding artifacts representing false information (Chandler and Roberson 2009).

In time-lapse experiments it is possible to make movies that can provide astonishing information about the dynamics of labelled structures or macromolecules in living fungal cells. The number of images is only limited by computer memory, with time intervals generally from 0.5 s to 1 min. A set of images in a time-lapse series can be further processed (contrast changed, brightness changed, cropped, and merged) and saved as a format appropriate for movie-making software (e.g., Adobe Premier®, Quicktime®), most commonly *.avi and *.mov. With the movie-making software, proprietary or not, movies can be accelerated, compressed, edited, and labeled for further presentation. For additional information on these topics see Chandler and Roberson (2009) and Umbaugh (2011).

1.11 Frequently Asked Questions

1.11.1 Do Vital Fluorescent Dyes Work Equally Well for Live-Cell Imaging of All Fungal Species and Cell Types?

Imaging live cells with confocal microscopy that have incorporated vital fluorescent dyes requires using dyes at concentrations that are noncytotoxic and unharmful levels of laser radiation (Hickey et al. 2005); two considerations that can vary between organisms and cell types. Thus, the answer to the question is no; one must consult the literature for previously published protocols or empirically determine what staining and imaging conditions work the best for any given specimen. The bottom line for this and all live-cell imaging is to handle samples gently, making sure they maintain viability and health.

1.11.2 How to Test Cell Viability After Staining?

The use of single or combined dyes can result in cell death, making it important to test the viability of fungal cells following staining prior to live-cell imaging. Staining with fluorescein (live cells) and propidium iodide (dead cells) simultaneously can be used to quantify percentage survival (Oparka and Read 1994). When there is a low percentage of survival, it is important to search for an alternative dye, method, or dye concentration.

1.11.3 How to Assess the Fitness of Living Cells?

The use of certain vital fluorescent probes (e.g., FM4-64), high laser power, or simply contact with the glass cover slip can perturb the cells and interfere with live-cell imaging. It is important to note any cellular perturbations, for example, in hyphae

reduced growth rate, swelling or narrowing of the hyphal tip, retraction or disappearance of the Spitzenkörper, and changes in organelle morphology and/or cytoplasmic distribution. Some of these perturbations can be prevented by incubating the sample in an appropriate growth medium for several minutes before performing live-cell imaging (Hickey et al. 2002).

1.11.4 How to Reduce Photobleaching?

Photobleaching is one of the greatest challenges of confocal microscopy, but not as severe as that in wide-field epifluorescence microscopy that uses a different source of illumination that cannot be readily tuned (Shotton 1989). There are differences in both the stability and quenching of the various fluorophores currently available. Undesirable photobleaching can be reduced by minimizing laser intensity or by using longer intervals between scans. The latter solution is not viable if events must be tracked quickly, but it is important to find the balance between scan time, interval between scans, and the time scale of the event to be recorded. Other variables that can influence photobleaching are pinhole size, detector sensitivity, NA of the objective lens, and level of magnification.

1.11.5 What to Do When a Staining Protocol That Normally Works Fails?

A protocol that produces good results can sometimes cease to work, which will relate either to the confocal system or the specimen. It is always good practice to first screen the specimen on a conventional epifluorescence microscope to evaluate sample preparation. If epifluorescence is visible, then a known specimen should also be imaged with the confocal using standard parameters, such as laser power, pinhole diameter, objective lens, field of view, gain, and black level of the detector. The latter is also good practice prior to imaging a new specimen. If there is a problem with the confocal system and the user is unsure of how to proceed, it is best to request technical support from the microscope manufacturer.

1.11.6 How to Deal with Bleed-Through in Multi-labeled Specimens?

For multi-labeled specimens, there can be bleed-through from one detection channel to another that can result from overlapping fluorescence spectra, Förster resonance energy transfer, or a limited number of emission filters. As mentioned before, it is possible to collect the spectral curve of each fluorophore in the context of single-labeled strains and use the information as a reference for a multi-labeled specimen. Some confocal systems have sufficient filters and PMTs to allow the user

to define the specific wavelength range of each channel. In this way, the user can select a narrow range associated with the emission maximum for each fluorophore to distinguish the different signals. If such a system is not available, most confocal systems offer software options that deconvolve spectral curves post data collection; alternatively, single detection channels can be collected sequentially.

1.11.7 How to Deal with Background and Autofluorescence?

Autofluorescence occurs naturally in many fungal cells from intrinsic fluorophores (e.g., aromatic amino acids, NADH, FAD, and pyridoxal phosphate) and can be a major source of background interference during imaging. Also certain reagents, such as fixatives (e.g., glutaraldehyde) and culture media components can introduce background fluorescence. Thus, before staining, it is important to observe an unstained specimen at different wavelengths with low laser power and black-level detector settings to identify autofluorescence and background fluorescence. There are specific compounds that can diminish autofluorescence (e.g., sodium borohydride) (Beisker et al. 1987), or fluorophores can be excited at wavelengths longer than (usually visible) autofluorescence (often UV). Another approach to deal with autofluorescence is to remove the signal using digital image-processing techniques such as image subtraction, ideally after having collected images from an unlabelled sample. Spectral imaging methods (see above) can also be applied to minimize autofluorescence. Impure immersion oil used for high-resolution imaging will cause background fluorescence, necessitating fluorescence-free oil for all fluorescence-based microscopies.

1.12 Conclusion

In the past 20 years, there has been a widespread interest in confocal microcopy. This has resulted in considerable improvement in all the optical and electronic components of this bioimaging approach and in the development of a large number of vital fluorescent probes, particularly for imaging live biological specimens. The resolution of confocal microscopy has been proven to be superior to wide-field epifluorescence microscopy. Nevertheless, the full potential of LSCM is yet to come—the idea is to use LSCM for single cell or even single molecule biochemical experiments. A major improvement would be enhancing the ability of LSCM to follow macromolecular intracellular reactions and dynamics, and establish the relationship between specific macromolecules within subcellular compartments.

LSCM is a very powerful tool, versatile, easy to use, and has become a common bioimaging method for many academic and industrial laboratories worldwide. Fungal scientists have found confocal microscopy to be an invaluable tool in addressing broad questions concerning fungal cell biology, from intracellular signaling to cytoplasmic organization and dynamics (Czymmek et al. 1994; Hickey and Read

2009). LSCM requires a wide range of skills, including the ability to operate complex computer software, an understanding of light microscopy optics, and a detailed knowledge of the biology of the system under study. Although, confocal images can be easily obtained, LSCM requires a broad range of skills to take full advantage of the technique. A better understanding of the various technologies involved in LSCM helps to produce more reliable data, and graduate from a "pretty picture" to an "elucidating image" (Hibbs 2004).

References

Ackermann GK, Eichler J (2007) Holography—a practical approach. Wiley, Weinheim

Amos WB, White JG (2003) How the confocal laser scanning microscope entered biological research. Biol Cell 95:335–342

Arcangeli C, Yu W, Cannistraro S, Gratton E (2000) Two-photon autofluorescence microscopy and spectroscopy of Antarctic fungus: new approach for studying effects of UV-B irradiation. Biopolymers 57:218–225

Atkinson HA, Daniels A, Read ND (2002) Live-cell imaging of endocytosis during conidial germination in the rice blast fungus, *Magnaporthe grisea*. Fungal Genet Biol 37:233–244

Bacia K, Kim SA, Schwille P (2006) Fluorescence cross-correlation spectroscopy in living cells. Nat Meth 3:83–89

Beisker W, Dolbeane F, Gray JW (1987) An improved immunocytochemical procedure for high-sensitivity detection of incorporated bromodeoxyuridine. Cytometry 8:235–239

Betz WJ, Mao F, Bewick GS (1992) Activity-dependent fluorescent staining and destaining of living vertebrate motor nerve terminals. J Neurosci 12:363–375

Betz WJ, Mao F, Smith CB (1996) Imaging exocytosis and endocytosis. Curr Opin Neurobiol 6:365–371

Bielska E, Higuchi Y, Schuster M, Steinberg N, Kilaru S, Talbot NJ, Steinberg G (2014) Long-distance endosome trafficking drives fungal effector production during plant infection. Nat Commun. doi:10.1038/ncomms6097

Bolte S, Talbot C, Boutte Y, Catrice O, Read ND, Satiat-Jeunemaitre B (2004) FM-dyes as experimental probes for dissecting vesicle trafficking in lving plant cells. J Microsc 214:159–173

Bourett TM, Czymmek KJ, Howard RJ (1998) An improved method for affinity probe localization in whole cells of filamentous fungi. Fungal Genet Biol 24:3–13

Bowman BJ, Draskovic M, Freitag M, Bowman EJ (2009) Structure and distribution of organelles and cellular location of calcium transporters in *Neurospora crassa*. Eukaryot Cell 8:1845–1855. doi:10.1128/EC.00174–09

Byer R (1988) Diode laser—pumped solid-state lasers. Science 239(4841):742–747. doi:10.1126/science.239.4841.742

Caballero-Lima D, Sudbery PE (2014) In *Candida albicans*, phosphorylation of Exo84 by Cdk1-Hgc1 is necessary for efficient hyphal extension. Mol Biol Cell 25:1097–1110

Chandler DE, Roberson RW (2009) Bioimaging: current concepts in light and electron microscopy, 1st edn. Jones and Bartlett Publishers LLC, Sudbury

Cochilla AJ, Angelson JK, Betz WJ (1999) Monitoring secretory membrane with FM1-43 fluorescence. Annu Rev Neurosci 22:1–10

Conchello JA, Lichtman JW (2005) Optical sectioning microscopy. Nat Methods 2:920–931

Czymmek KJ (2005) Exploring fungal activity with confocal and multiphoton microscopy. In Dighton J, White JF, Oudemans P (eds) The fungal community: its organization and role in the ecosystem, 3rd edn. CRC Press, Boca Raton

Czymmek KJ, Whallon JH, Klomparens A (1994) Confocal microscopy in mycological research. ExpMycol 18:275–293

Czymmek KJ, Fogg M, Powell DH, Sweigard J, Park SY, Kang S (2007) In vivo time-lapse documentation using confocal and multi-photon microscopy reveals the mechanisms of invasion into the Arabidopsis root vascular system by *Fusarium oxysporum*. Fungal Genet Biol 44:1011–1023

Day RD, Davidson MW (2009) The fluorescent protein palette: tools for cellular imaging. Chem Soc Rev 38:2887–2921. doi:10.1039/B901966A

Delgado-Álvarez DL, Callejas-Negrete OA, Gómez N, Freitag M, Roberson RW, Smith LG, Mouriño-Pérez RR (2010) Visualization of F-actin localization and dynamics with live cell markers in *Neurospora crassa*. Fungal Genet Biol 47:573–586

Delgado-Álvarez DL, Bartnicki-García S, Seiler S, Mouriño-Pérez RR (2014) Septum development in *Neurospora crassa*: the Septal Actomyosin Tangle. PLoS One 9(5):e96744

Diaspro A (2001) Confocal and two-photon microscopy: foundations, applications, and advances. Wiley-Liss, New York

Digman MA, Gratton E (2009) Fluorescence correlation spectroscopy and fluorescence cross-correlation spectroscopy. Wiley Interdiscip Rev Syst Biol Med 1:273–282

Dijksterhuis J (2003) Confocal microscopy of Spitzenkörper dynamics during growth and differentiation of rust fungi. Protoplasma 222:53–59

Elorza MV, Rico H, Sentandrew R (1983) Calcofluor white alters the assembly of chitin fibirls in *Saccharomyces cerevisiae* and *Candida albicans* cells. J Gen Microbio 129:1577–1582

Epp E, Nazarova E, Regan H, Douglas LM, Konopka JB, Vogel J, Whiteway M (2013) Clathrin- and Arp2/3-independent endocytosis in the fungal pathogen *Candida albicans*. mBio 4:e00476–e00413. doi:10.1128/mBio.00476–13

Feijo JA, Moreno N (2004) Imaging plant cells by two-photon excitation. Protoplasma 223:1–32

Fisher-Parton S, Parton RM, Hickey PC, Dijksterhuis J, Atkinson HA, Read ND (2000) Confocal microscopy of FM4-64 as a tool for analyzing endocytosis and vesicle trafficking in living fungal hyphae. J Microsc 198:246–259

Foldes-Papp Z, Demel U, Tilz GP (2003) Laser scanning confocal fluorescence microscopy: an overview. Int Immunopharmacol 3:1715–1729

Freitag M, Selker EU (2005) Expression and visualization of red fluorescent protein (RFP) in *Neurospora crassa*. Fungal Genet Newslett 52:14–17

Freitag M, Ciuffetti LM, Selker EU (2001) Expression and visualization of green fluorescent protein (GFP) in *Neurospora crassa*. Fungal Genet Newslett 48:15–19

Freitag M, Hickey PC, Raju NB, Selker EU, Read ND (2004) GFP as a tool to analyze the organization, dynamics and function of nuclei and microtubules in *Neurospora crassa*. Fungal Genet Biol 41(10):897–910

Fuchs F, Prokisch H, Neupert W, Westermann B (2002) Interactions of mitochondria with microtubules in the filamentous fungus *Neurospora crassa*. J Cell Sci 115:1931–1937

Haase J, Mishra PF, Stephens A, Haggerty R, Quammen C, Taylor RM, Yeh E, Basrai MA, Bloom K (2013) A 3D map of the yeast kinetochore reveals the presence of core and accessory centromere-specific histone. Curr Biol 23:1939–1944

Haraguchi T, Shimi T, Koujin T, Hashiguchi N, Hiraoka Y (2002) Spectral imaging fluorescence microscopy. Genes Cells 7:881–887

Hibbs AR (2004) Confocal microscopy for biologists. Springer, New York

Hickey PC, Read ND (2003) Biology of living fungi. British Mycological Society, Stevenage. (CD–ROM)

Hickey PC, Read ND (2009) Imaging living cells of *Aspergillus* in vitro. Med Mycol 47(Supplement 1):S110–S119

Hickey PC, Jacobson DJ, Read ND, Glass NL (2002) Live-cell imaging of vegetative hyphal fusion in *Neurospora crassa*. Fungal Genet Biol 37:109–119

Hickey PC, Swift SR, Roca MG, Read ND (2005) Live-cell imaging of filamentous fungi using vital fluorescent dyes and confocal microscopy. Method Microbio 34:63–87. doi:10.1016/S0580-9517(04)34004-1

Hiraoka Y, Shimi T, Hashiguchi N (2002) Multispectral imaging fluorescence microscopy for living cells. Cell Struct Func 27:367–374

Hoch HC, Staples RC (1985) The microtubule cytoskeleton in hyphae of *Uromyces phaseoli* germlings: its relationship to the region of nucleation and to the F-actin cytoskeleton. Protoplasma 124:112–122

Hoffman J, Mendgen K (1998) Endocytosis and membrane turnover in the germ tube of *Uromyces fabae*. Fungal Genet Biol 24:77–85

Huang B, Bates M, Zhuang X (2009) Super resolution fluorescence microscopy. Annu Rev Biochem 78:993–1016. doi:10.1146/annurev.biochem.77.061906.092014

Hwang LC, Wohland T (2007) Recent advances in fluorescence cross-correlation spectroscopy. Cell Biochem Biophys 49:1–13

Hyde GJ, Hardham AR (1992) Confocal microscopy of microtubule arrays in cryosectioned sporangia of *Phytophthora cinnamomi*. ExpMycol 16:201–218

Ichiwara A, Tanaami T, Ishida H, Shimizu M (1999) Confocal fluorescent microcopy using a Nipkow scanner. In: Mason WT (ed) Fluorescent and luminescent probes for biological activity, 2nd edn. Academic, San Diego, pp 344–349

Johnson LV, Walsh ML, Chen LB (1980) Localization of mitochondria in living cells with rhodamine 123. Proc Natl Acad Sci U S A 77:990–994

Knaus H, Blab GA, Agronskaia AV, van den Heuvel DJ, Gerritsen HC, Wösten HAB (2013) Monitoring the metabolic state of fungal hyphae and the presence of melanin by nonlinear spectral imaging. Appl Environ Microbiol 79:6345–6350

Knight H, Trewavas AJ, Read ND (1993) Confocal microscopy of living fungal hyphae microinjected with Ca^{2+}-sensitive fluorescent dyes. Mycol Res 97:1505–1515

Koechner W (2006) Solid-state laser engineering, vol. 1. 6th, rev. and updated ed. Springer, Berlin

Köhli M, Galati V, Boudier V, Roberson RW, Philippsen P (2008) Growth-speed correlated localization of exocyst and polarisome components in growth zones of *Ashbya gossypii* hyphal tips. J Cell Sci 121:3803–3814

Koll F, Sidoti C, Rincheval V, Lecellier G (2001) Mitochondrial membrane potential and ageing in *Podospora anserina*. Mech Ageing Dev 122:205–217

König K (2000) Multiphoton microscopy in life sciences. J Microsc 200:83–104

Krichevsky O, Bonnet G (2002) Fluorescence correlation spectroscopy: the technique and its applications. Rep Prog Phys 65:251–297

Kurtsiefer C, Mayer S, Zarda P, Weinfurter H (2000) Stable solid-state source of single photons. Phys Rev Lett 85:290

Leith EN, Upatnieks J (1963) Wavefront reconstruction with continuous-tone objects. J Opt Soc Am 53(12):1377–1381

Leith EN, Upatnieks J (1964) Wavefront reconstruction with diffused. J Opt Soc Am 54(11):1295–1301

Leroch M, Mernke D, Koppenhoefer D, Schneider P, Mosbach A, Doehlemann G, Hahn M (2011) Living colors in the gray mold pathogen *Botrytis cinerea*: codon-optimized genes encoding green fluorescent protein and mcherry, which exhibit bright fluorescence. Appl Environ Microbiol 77(9):887–2897. doi:10.1128/AEM.02644–10

Lin S-J, Tan H-Y, Kuo C-J, Wu R-J, Wang S-H, Chen W-L, Jee S-H, Dong C-Y (2009) Multiphoton autofluorescence spectral analysis for fungus imaging and identification. Appl Phys Lett 95:43703–43703. doi:10.1063/1.3189084

Lowry D, Roberson RW (1997) The microtubule cytoskeleton during zoospore formation in *Allomyces macrogynus*. Protoplasma 196:45–54

McDaniel DP, Roberson RW (1998) γ-Tubulin is a component of the Spitzenkörper and centrosomes in hyphal tip cells of *Allomyces macrogynus*. Protoplasma 203:118–123

McDaniel DP, Roberson RW (2000) Microtubules are required for motility and positioning of vesicles and mitochondria in hyphal tip cells of *Allomyces macrogynus*. Fungal Genet Biol 31(3):233–244

Minsky M (1988) Memoir on inventing the confocal scanning microscope. Scanning 10:128–138

Miyawaki A (2003) Fluorescence correlation spectroscopy for the detection and study of single molecules in biology. Bioessays 24:758–764

Murphy DB, Davidson MW (2013) Fundamentals of light microscopy and electronic imaging. 2nd ed. Wiley, Hoboken

Murray JM, Appleton PL, Swedlow JR, Waters JC (2007) Evaluating performance in three dimensional fluorescence microscopy. J Microsc 228:390–405
Nakano A (2002) Spinning-disk confocal microscopy-a cutting-edge tool for imaging of membrane traffic. Cell Struct Func 27:349–355
Nasse MJ, Woehl JC (2010) Realistic modeling of the illumination point spread function in confocal scanning optical microscopy. J Opt Soc Am A 27(2):295–302. doi:10.1364/JOSAA.27.000295
Oparka KJ, Read ND (1994) The use of fluorescent probes for studies on living plant cells. In Harris N, Oparka KJ (eds) Plant cell biology. A practical approach. IRL Press, Oxford
Paddock SW (2000) Principles and practices of laser scanning confocal microscopy. Mol Biotech 16:127–149
Paddock SW (2008) Over the rainbow: 25 years of confocal imaging. Bio Techniques 44:643–648
Panepinto J, Komperda K, Frases S, Park YD, Djordjevic JT, Casadevall A, Williamson PR (2009) Sec6-dependent sorting of fungal extracellular exosomes and laccase of *Cryptococcus neoformans*. Mole Micro 71:1165–1176
Pawley JB (2006) Handbook of biological confocal microscopy, 3th ed. Plenum Press, New York
Pawley JB (2010) Handbook of biological confocal microscopy (Google eBook). Springer, New York
Rasmussen CG, Glass NL (2007) Localization of RHO-4 indicates differential regulation of conidial versus vegetative septation in the filamentous fungus *Neurospora crassa*. Eukaryot Cell 6:1097–1107
Read ND, Hickey PJ (2001) The vesicle trafficking network and tip growth in fungal hyphae. In: Geitmann A, Cresti M, Heath IB (eds) Cell biology of plant and fugal tip growth. IOS Press, Amsterdam
Read ND, Kalkman ER (2003) Does endocytosis occur in fungal hyphae? Fungal Genet Biol 39:199–203
Riedl J, Crevenna AH, Kessenbrock K, Yu JH, Neukirchen D, Bista M, Bradke F, Jenne D, Holak TA, Werb Z, Sixt M, Wedlich-Söldner R (2008) Lifeact: a versatile marker to visualize F-actin. Nat Methods 5:605–607
Rines DR, Thomann D, Dorn JF, Goodwin P, Sorger PK (2011) Live cell imaging of yeast. Cold Spring Harb Protoc 9:pdb.top065482
Riquelme M, McDaniel DP, Roberson RW, Bartnicki-García S (2002) The effect of ropy-1 mutation on cytoplasmic organization in mature hyphae of *Neurospora crassa*. Fungal Genet Biol 37:171–179
Roberson RW (1992) The actin cytoskeleton in hyphal cells of *Sclerotium rolfsii*. Mycologia 84:41–51
Roncero C, Duran A (1985) Effect of calcoflúor white and congo red on fungal wall morphogenesis: in vivo activation of chitin polymerization. J Bacteriol 170:1950–1954
Shen KF, Osmani SA (2013) Regulation of mitosis by the NIMA kinase involves TINA and its newly discovered partner An-WDR8, at spindle pole bodies. Mol Biol Cell 24:3842–3856
Sheppard CJR, Shotton DM (1997). Confocal laser scanning microscopy. IOS Scientific Publishers, Oxford
Shotton DM (1989) Confocal scanning optical microscopy and its applications for biological specimens. J Cell Sci 94:175–206
Steinber G, Schliwa M, Lehmler C, Bölker M, Kahmann R, McIntosh JR (1998) Kinesin from the plant pathogenic fungus *Ustilago maydis* is involved in vacuole formation and cytoplasmic migration. J Cell Sci 111:2235–2246
Svelto O, Hanna DC (1989) Principles of lasers, 3rd edn. Plenum, New York, p. 494
Swedlow JR (2003) Quantitative fluorescence microscopy and image deconvolution. Meth Cell Biol 72:346–367
Szewczyk E, Oakley BR (2011) Microtubule dynamics in mitosis in *Aspergillus nidulans*. Fungal Genet Biol 48(10):998–999
Tcherniak A, Reznik C, Link S, Landes CF (2009) Fluorescence correlation spectroscopy: criteria for analysis in complex systems. AnalytChem 81:746–754
Thorn K (2010) Spinning-disk confocal microscopy of yeast. Meth Enzmol 470:581–602

Torralba S, Heath IB (2002) Analysis of three separate probes suggests the absence of endocytosis in *Neurospora crassa* hyphae. Fungal Genet Biol 37:221–232

Tsujia T, Kawai-Nomaa S, Packb C-G, Terajimaa H, Yajimac J, Nishizakac T, Kinjod M, Taguchia H (2011) Single-particle tracking of quantum dot-conjugated prion proteins inside yeast cells. Biochem Bioph Res Co 405(4):638–643

Umbaugh SE (2011) Digital image processing and analysis. CRC Press, Boca Raton

Vida TA, Emr SD (1995) A new vital stain for visualizing vacuolar membrane dynamics and endocytosis in yeast. J Cell Biol 128:779–792

Wallace W, Schaefer LH, Swedlow JR (2001) A workingperson's guide to deconvolution in light microscopy. Biotechniques 31(5):1076–1078

Wang E, Babbey CM, Dunn KW (2005) Performance comparison between the high-speed Yokogawa spinning disc confocal system and single-point scanning confocal systems. J Microsc 218:148–59

Waterman-Storer CM, Shaw SL, Salmon ED (1997) Production and presentation of digital movies. Trends Cell Biol 7:503–506

Wokosin DL, Centonze VE, Crittenden S, White J (1996) Three-photon excitation fluorescence imaging of biological specimens using an all-solid-state laser. Bioimaging 4:208–214

Woyke T, Winkelmann G, Roberson RW, Pettit GR, Pettit RK (2002) Three-dimensional visualization of microtubules during the *Cryptococcus neoformans* cell cycle and effects of auristatin PHE. Antimicrob Agents Chemother 46:3802–3808

Yaffe MP, Stuurman N, Vale RD (2003) Mitochondrial positioning in fission yeast is driven by association with dynamic microtubules and mitotic spindle poles. Proc Natl Acad Sci U S A. 100:11424–8

Zekert N, Fischer R (2009) The *Aspergillus nidulans* kinesin-3 uncA motor moves vesicles along a subpopulation of microtubules. Mol Biol Cell 20:673–684